Electronic Supplementary Material (ESI) for Journal of Materials Chemistry A.


Electronic Supporting Information (ESI):

# Band gap narrowing of $SnS_2$ superstructures with improved hydrogen production

Guowei Li,[a] Ren Su,[b,c] Jiancun Rao,[d] Jiquan Wu,[a] Petra Rudolf,[a] Graeme R. Blake,[a] Robert A. de Groot, [a,e] Flemming Besenbacher,[b] and Thomas T. M. Palstra*[a]

a. Zernike Institute for Advanced Materials, University of Groningen, Nijenborgh 4, 9747 AG Groningen, The Netherlands.

b. Interdisciplinary Nanoscience Center, Aarhus University, Gustav Wieds Vej 14, DK-8000 Aarhus C, Denmark.

c. Syncat @Beijing, Synfuels China Co. Ltd., Leyuan South, Street II, No.1, Yanqi Economic Development Zone C# Huairou District, Beijing, 101407, P. R. China

d. School of Materials Science and Engineering, Harbin Institute of Technology, 150001 Harbin, PR China.

e. Institute for Molecules and Materials, Radboud University Nijmegen, Heyendaalseweg 135, 6525 AJ Nijmegen, The Netherlands

***Characterization*:** X-ray diffraction (XRD) patterns were recorded with a Bruker D8 Advance diffractometer equipped with a Cu Kα source (λ= 0.15406 nm, 40 kV, 40 mA). The step-scanned XRD data were recorded in the range 20-80° 2$\theta$ with a 0.02° step size. Rietveld refinements of the diffraction data were performed using the GSAS and EXPGUI suite of programs.[1] The morphology and crystal structure were examined using a Philips XL 30 scanning electron microscope (SEM) and a JEM 2010F transmission electron microscope (TEM) operated at an accelerating voltage of 200 KV. The $N_2$ adsorption/desorption isotherms were measured using a surface area analyzer (Nova e2000, Quantachrome) to determine the specific surface area by the Brunauer–Emmett–Teller (BET) theory. Prior to analysis, the as-synthesized $SnS_2$ was degassed at 373 K for three hours under dynamic vacuum conditions to remove surface adsorbed water. XPS data were collected by using a surface science SSX-100 ESCA instrument equipped with a monochromatic A1 Kα X – Ray source (h$\nu$ = 1486.6 eV) and operating at a base pressure of 1 x $10^{-9}$ mbar. The spectra were recorded with an electron take – off angle of 37° with respect to the surface normal on a spot with a diameter of 1000 μm. The energy resolution was set to 1.26 eV. The spectra were analysed using the least-squares curve fitting program Winspec developed at the LISE laboratory, University of Namur, Belgium. Binding energies are reported to a precision of ± 0.1 eV and referenced to element S. Deconvolution of the spectra included a Shirley background subtraction and fitting with a minimum number of peaks, taking into account the experimental resolution. The profile of the peaks was taken as a convolution of Gaussian and Lorentzian functions. The uncertainty in the peak intensity determination was 3% for sulfur, and 2% for Sn. All measurements were carried out on freshly prepared samples. Three different spots were measured on each surface to check for reproducibility.

| Sample | $FeS_2$, $SnS_2$, CuS, $Ni_3S_4$ | $FeS_2/Fe_7S_8$ | $SnS_2/SnS$ | CuS@C |
|---|---|---|---|---|
| $CS_2$ (mL) | 16 | 20 [a)] | 20 | 16 |
| Ethanol (mL) | 16 | 15 | 12 | 16 |

a) Methanol was used in this case

**Table S1.** Solvent ratios for the synthesis of metal sulfide superstructures

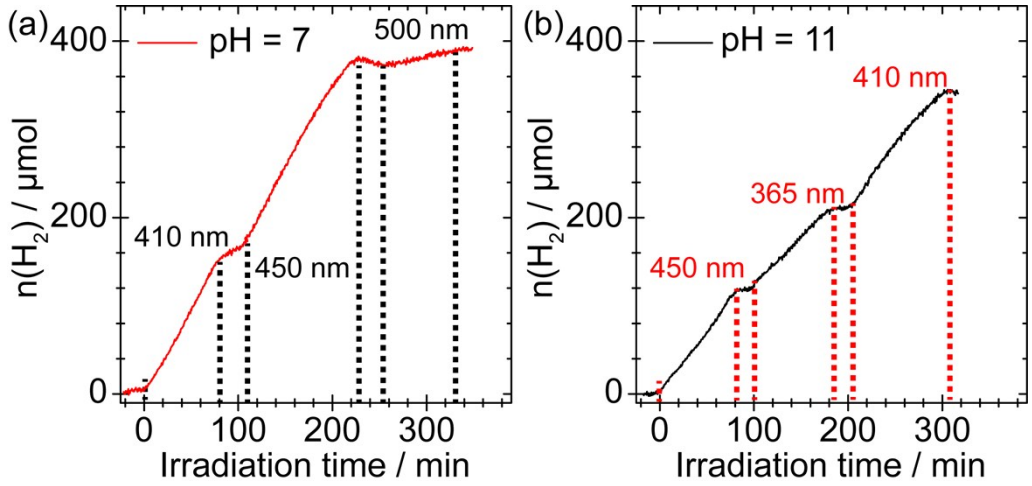


**Figure S1** Stability tests of the $SnS_2$ sample as photocatalyst at pH 7 (a) and pH 11 (b), respectively.

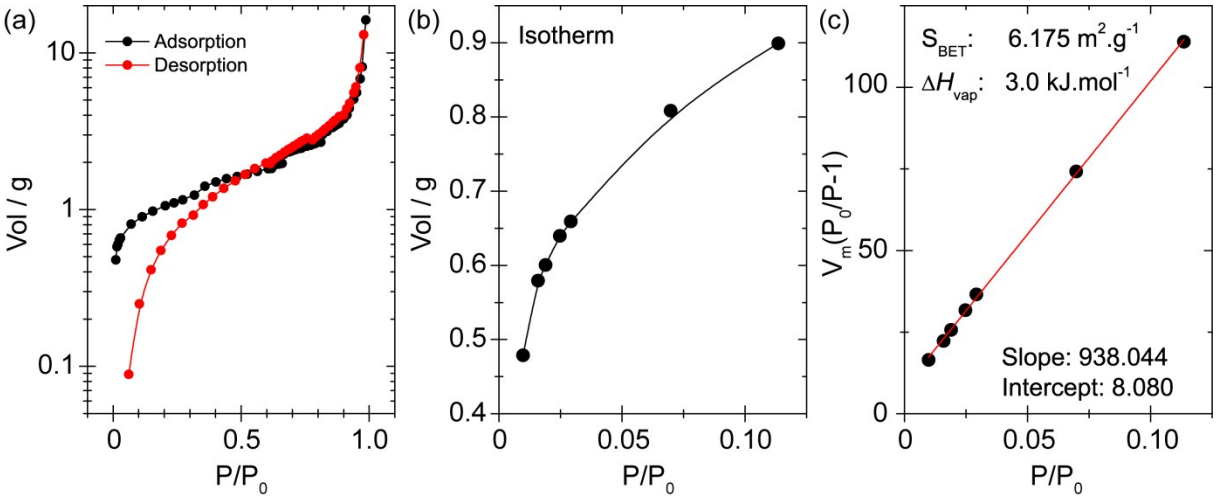


**Figure S2** (a) $N_2$ adsorption and desorption isotherms of as-synthesized $SnS_2$. (b) $N_2$ adsorption isotherm used for (c) the determination of BET surface area.

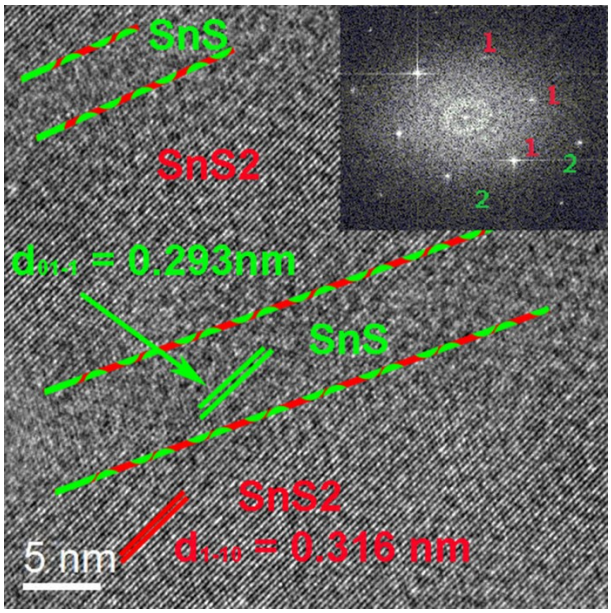


**Figure S3** HRTEM image of a nanoplate showing the alternating blocks of $SnS_2$/SnS; the inset shows the corresponding FFT pattern.

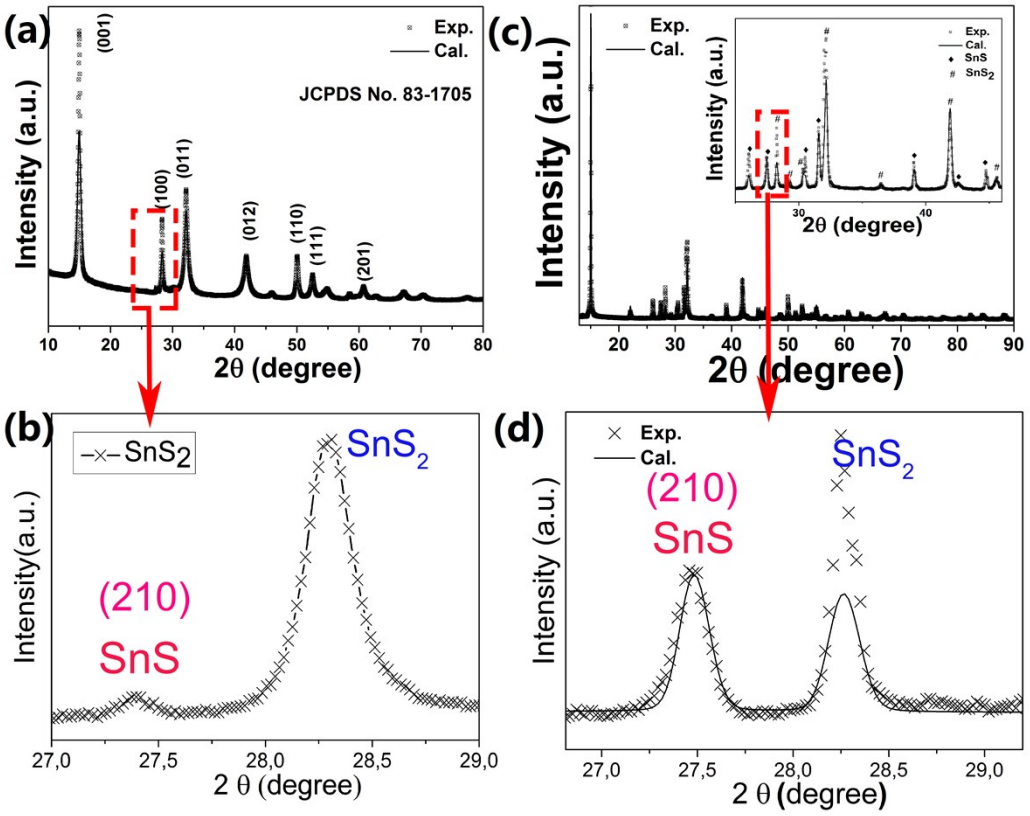


**Figure S3** (a) XRD patterns of SnS microspheres and (b) the magnified region between 27- 29°. (c) XRD patterns of $SnS_2$/SnS composite and (b) the magnified region between 27-29°.

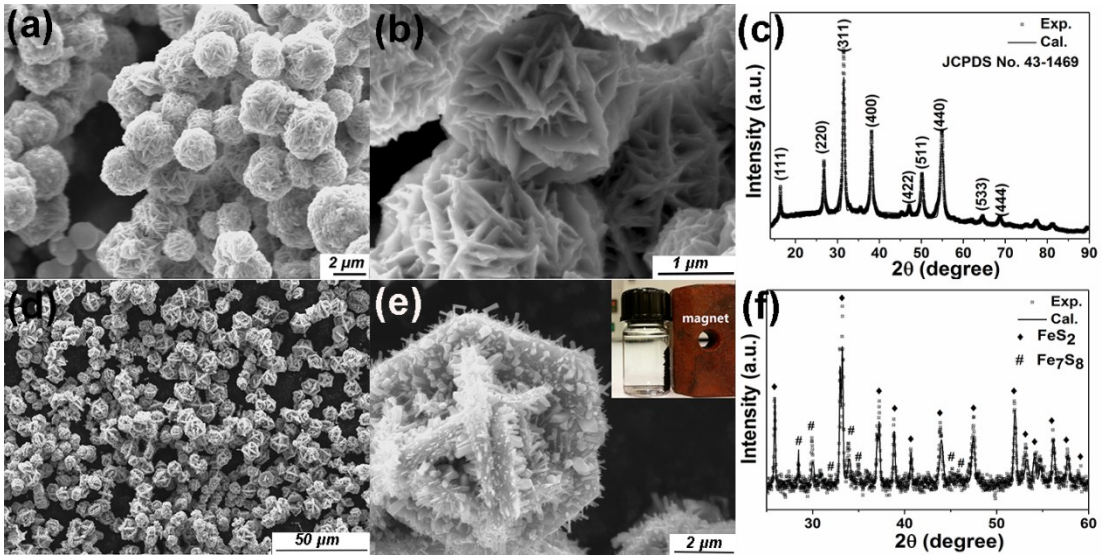


**Figure S5** SEM images of as-prepared $Ni_3S_4$ (a and b) and $FeS_2/Fe_7S_8$ (d and e) 3 D hierarchical structures. The inset shows the magnetic separation of $FeS_2/Fe_7S_8$ crystals from ethanol solution using a magnet. (c) and (f) show the corresponding observed (data points) and calculated (solid line) XRD patterns of the as-prepared samples.

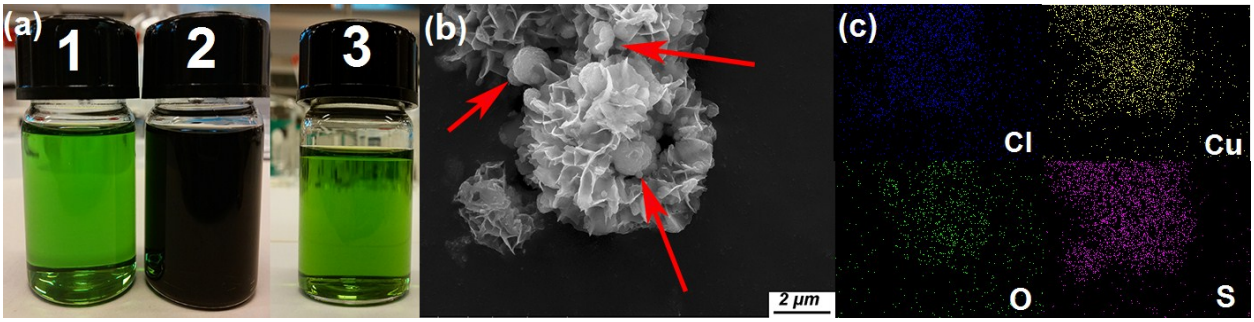


**Figure S6** (a) Color of CuS reaction solutions at different stages: solution 1 is the fresh solution before heat treatment, solution 2 is after the temperature reached 180 ℃, and solution 3 is the same solution kept at room temperature for 2 days. (b) SEM image of a typical CuS structure with a reaction time of 20 minutes, and the corresponding elemental mapping of Cl, O, Cu, and S.

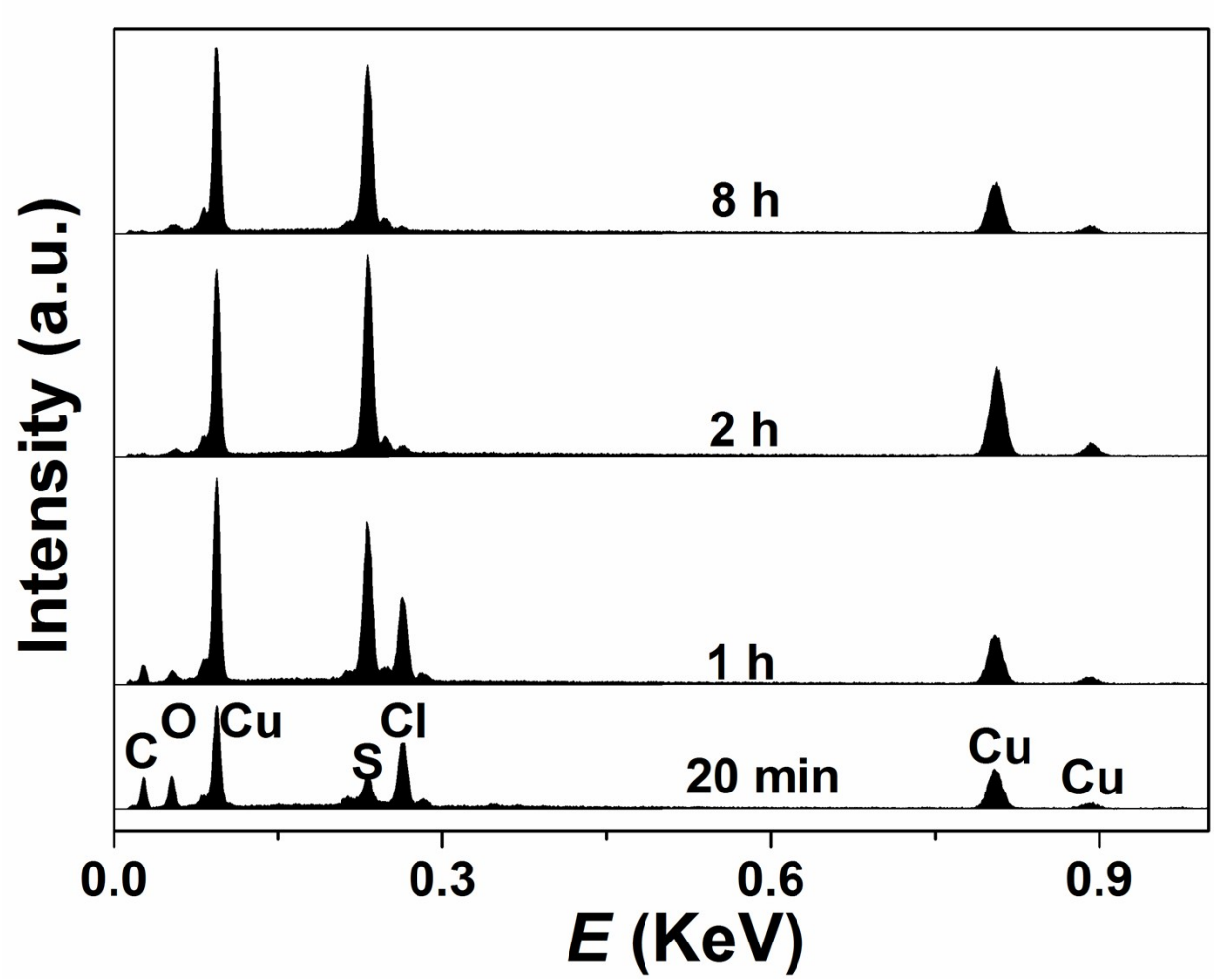


**Figure S7** EDS analysis of CuS obtained after reaction times of 20 min, slowly cooled down, 1h, 2h, 4 h, and 8 h.

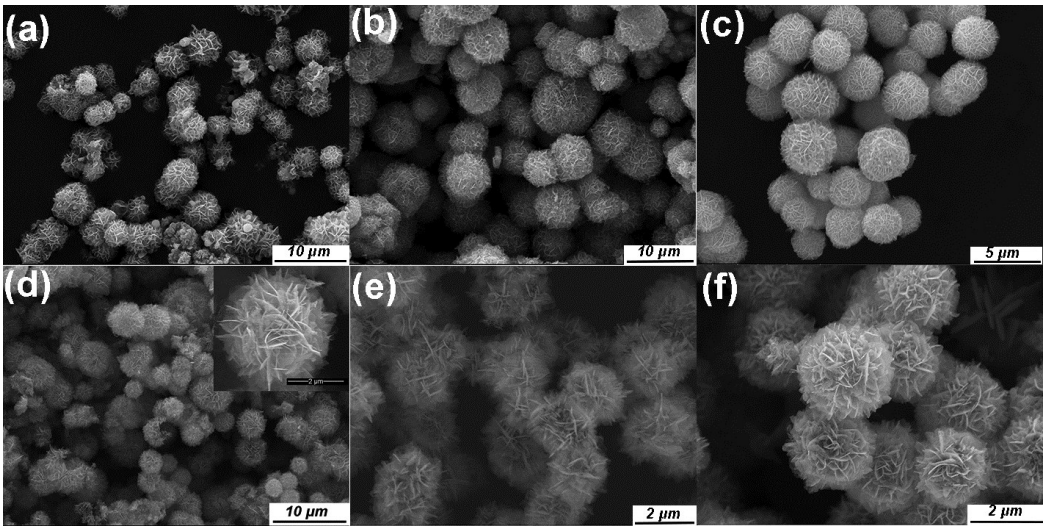


**Figure S8** SEM images of CuS obtained after reaction times of (a) 20 min, quickly cooled down, (b) 20 min, slowly cooled down, (c) 1h, (d) 2h, (e) 4 h, and (f) 8 h.

Light source characterization

A LED flash light (Optimax, Multi Lite, OFK-8000A, Spectroline) with interchangeable lamp heads was used as the light source with characteristic emission peaks at 365, 410, 450, and 500 nm, respectively. The light intensities of these lamp heads at 700 mA input are 310, 400, 480 mW, and 100 lumens according to the manufacture (http://www.spectroline.com/content/ofk-8000a-forensics).

In order to determine the quantum efficiency precisely, we characterised the 365 nm LED light and corrected the light intensities of 410 and 450 nm light relative to the 365 nm light. The emission spectrum of the 365 nm LED light source was measured by a spectrometer (HR4000CG-UV-NIR, Ocean optics) *via* an optical fibre (QP200-2-UV-BX), as shown in Fig. S7(A). The light source has a peak emission at 365 nm with a full-width-at-half-maximum (FWHM) of 10 nm. The photon flux of the light source was measured using a standard ferrioxalate actinometry method.

The photodecomposition of ferrioxalate shown in equation (1) has a well-defined quantum yield, and thus the number of absorbed photons in a certain volume of actinometer liquid can be precisely calculated.

$$2[Fe(C_2O_4)_3]^{3-} \rightarrow \ 2Fe^{2+} + 5C_2O_4^{2-} + 2CO_2 \quad (1)$$

In practice, the light intensity measurement was executed under dark red light conditions. 2 mL of the 130 mL actinometer solution (6 mM) subjected to various irradiation times, 2 mL of 0.1 wt% o-phenanthroline solution, 1 mL of buffer solution (0.6 M $CH_3COOH$ and 0.18 M $H_2SO_4$), and 15 mL deionised water were added to a 20 mL volumetric flask and mixed immediately. The mixture was developed in the dark for 1h to form the Fe(II)-1,10-phenanthroline complex, which presents a characteristic absorption maximum at 510 nm (Fig. S7B). The absorbance at 510 nm shows a linear correlation with the irradiation time (Fig. S3C), thus the photon flux (q) can be calculated using equation (2):

$$q = \Delta A/t \cdot (V_1 \cdot V_3/V_2) \cdot (N_A/\Phi_{Fe}^{2+} \cdot \varepsilon_{510nm} \cdot l) \quad (2)$$

where,

$\Delta A/t$ is the slope of the absorbance change with respect to time (shown in Fig. S7C);

$V_1$ is the total volume illuminated (130 mL);

$V_2$ is the aliquot volume (2 mL);

$V_3$ is the remaining volume of the liquid;

$N_A$ is Avogadro's number;

$\Phi_{Fe}^{2+}$ is the quantum yield of ferrioxalate at 365 nm (1.25 ± 0.02) [2];

$\varepsilon_{510nm}$ is the extinction coefficient of the Fe(II)-1,10-phenanthroline at 510 nm (11835.1 ± 28.9 $mol^{-1}L^{-1}cm^{-1}$);

l is the path length of light in the cuvette (1 cm).

Figure S7(D) depicts the calculated photon flux as a function of the irradiation time. The averaged photon flux is ~ 4 x $10^{17}$ photons /sec.

Since the light intensities of these lamp heads at 700 mA input are 310, 400, 480 mW, and the same power supply was used for all LED lamp heads, we assumed averaged photon fluxes of 5.5 x $10^{17}$ and 7.25 x $10^{17}$ photons·$s^{-1}$ for the 410 and 450 nm LEDs, respectively.

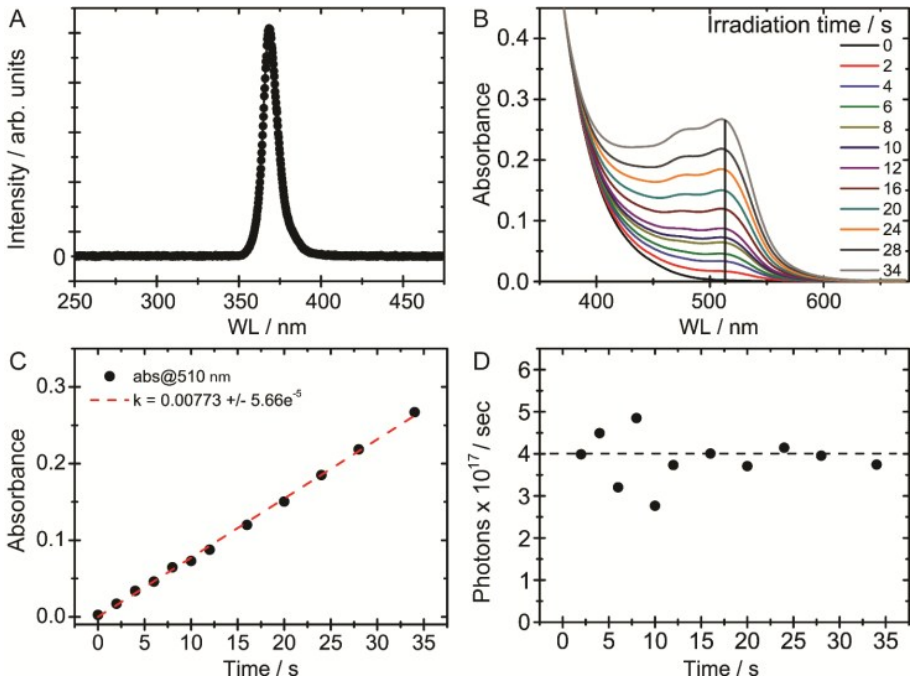


**Figure S9.** Characterisation of the OFK-8000A light source with a 365 nm head. (A) Light source emission spectra; (B) Ferrioxalate solution absorption spectrum under irradiation; (C) The absorbance of the ferrioxalate solution at 510 nm as a function of irradiation time; (D) Photon flux of the light source calculated from ferrioxalate actinometry analysis.

**Hydrogen evolution test, calibration, and MS spectra**

A mass spectrometry based hydrogen evolution test system was constructed and has been described previously.[2] The procedure used for hydrogen evolution has also been described previously.[3] The desired amount of fresh catalyst was transferred into a glass reactor and dispersed in deionised water. The desired amount of sacrificial reagent (ethanol) was then added to the reactor. The total liquid volume was always adjusted to be 25 mL. The mass spectrometer was switched on for two hours before starting the measurement in order to stabilise all signals for at least 20 minutes. The stabilisation process was carried out under an ambient pressure of air. The ratio of M/e = 28 to M/e = 32 obtained was 78:21, which agrees with the ratio of $p(N_2)$: $p(O_2)$ in air. The sum of these two partial pressures allows us to correlate the measured pressure of the vacuum chamber to the real pressure of the reaction chamber, which is necessary for further calibrations and quantitative calculations. The oxygen in the reaction chamber was pumping away using a bypass rotary pump. The chamber was then closed when the oxygen signal was stable for at least 5 minutes, and the light was switched on to initiate the photo-catalytic hydrogen evolution. During the reaction, typically $M/e^-$ values of 2, 15, 18, 28, 32, and 44 were monitored continuously, corresponding to the expected signals of hydrogen, methane, water, carbon monoxide, oxygen, and carbon dioxide respectively.

We calibrated the relative sensitivity factor (RSF) of hydrogen using a standard 5±0.1 vol% $H_2$ ($N_2$ as balance gas), as shown in Fig. S8(a). The four regions in the calibration process represent (I) mass spectrometer stabilization, (II) system evacuation and purging, (III) the calibration process, and (IV) venting, respectively. During the calibration, 0.5, 0.75, 0.9, and 1.25 bars of the gas were injected into the chamber in order to estimate the RSF. We performed the calibration twice and the ratio of 0.95 $pN_2$ to 0.05 $pH_2$ is plotted as a function of $pN_2$ in Fig.

S8(b). It can be seen that the ratio slightly decreases following an increase in $pN_2$, which indicates that the diffusion of $H_2$ is accelerated at higher pressures. Since the hydrogen evolution was carried out in low vacuum conditions, it is reasonable to apply an RSF of 1/2.5/1.41 (0.284) in vacuum.

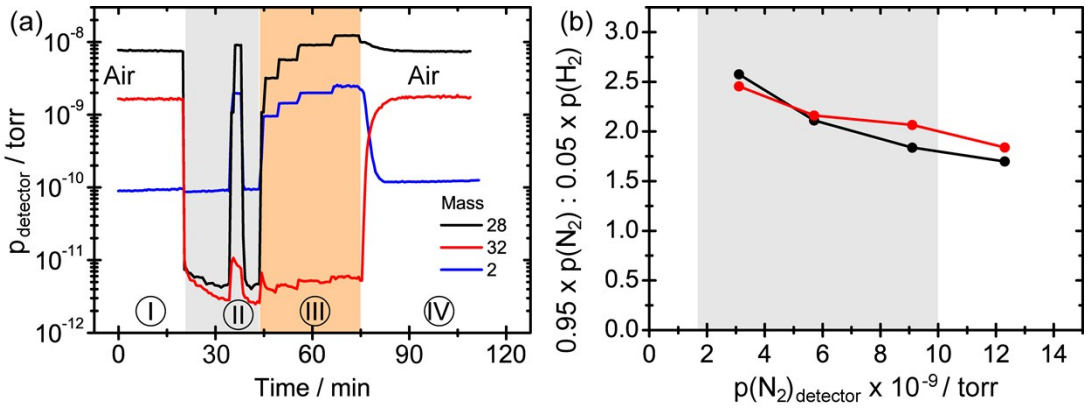


**Figure S10.** (a) Calibration of the relative sensitivity factor (RSF) using standard 5±0.1% $H_2$ gas. The balance gas is $N_2$. The four regions in (a) represent (I) mass spectrometer stabilization, (II) system evacuation and purging, (III) calibration process, and (IV) venting, respectively. (b) The ratio of $N_2/H_2$ as a function of the $pN_2$ conditions. The gray shaded region indicates the pressure range used in our hydrogen evolution experiments.

Both prior to and after the reaction, mass scans were also executed in order to identify the gas phase by-products, as shown in Fig. S9. No other species than $H_2$, $CH_4$, $H_2O$, $N_2$(CO), Ar, and $CO_2$ were observed, indicating that no reactions took place other than $H_2$ evolution from photocatalytic ethanol reforming.[4]

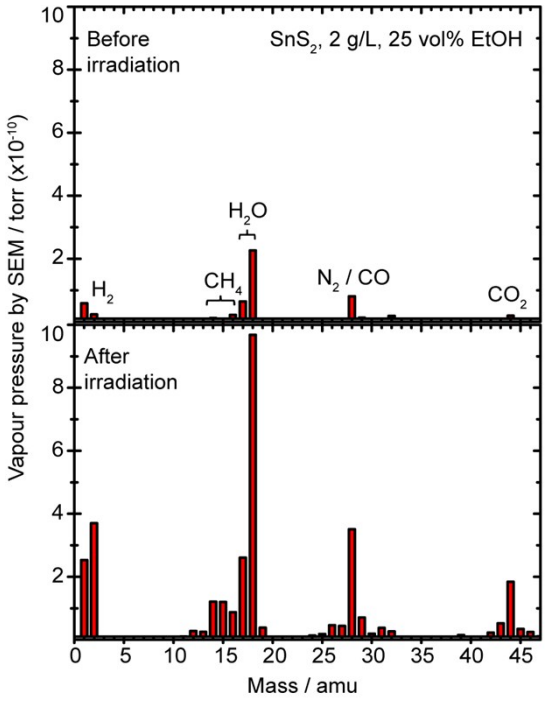


**Figure S11.** MS scan before and after irradiation.

## References


1. B. H. Toby, *J. Appl. Crystallogr.*, 2001, 34, 210-213.
2. R. Su, R. Tiruvalam, A. J. Logsdail, Q. He, C. A. Downing, M. T. Jensen, N. Dimitratos, L. Kesavan, P. P. Wells, R. Bechstein, H. H. Jensen, S. Wendt, C. R. Catlow, C. J. Kiely, G. J. Hutchings and F. Besenbacher, *ACS Nano*, 2014, 8, 3490-3497.
3. W. Jones, R. Su, P. P. Wells, Y. Shen, N. Dimitratos, M. Bowker, D. Morgan, B. B. Iversen, A. Chutia, F. Besenbacher and G. Hutchings, *Phys. Chem. Chem. Phys.*, 2014, 16, 26638-26644.
4. H. Bahruji, M. Bowker, P. R. Davies and F. Pedrono, *Appl. Catal. B-Environ.*, 2011, 107, 205-209.